

RELATIVITY AND THE EVOLUTION OF THE GALACTIC CENTER S-STAR ORBITS

FABIO ANTONINI

Canadian Institute for Theoretical Astrophysics, University of Toronto, 60 St. George Street, Toronto, Ontario M5S 3H8, Canada

DAVID MERRITT

Department of Physics and Center for Computational Relativity and Gravitation, Rochester Institute of Technology, 85 Lomb Memorial Drive, Rochester, NY 14623, USA

Draft version June 19, 2018

ABSTRACT

We consider the orbital evolution of the S-stars, the young main-sequence stars near the supermassive black hole (SBH) at the Galactic center (GC), and put constraints on competing models for their origin. Our analysis includes for the first time the joint effects of Newtonian and relativistic perturbations to the motion, including the dragging of inertial frames by a spinning SBH as well as torques due to finite- N asymmetries in the field-star distribution (resonant relaxation, RR). The evolution of the S-star orbits is strongly influenced by the Schwarzschild barrier (SB), the locus in the (E, L) plane where RR is ineffective at driving orbits to higher eccentricities. Formation models that invoke tidal disruption of binary stars by the SBH tend to place stars below (i.e., at higher eccentricities than) the SB; some stars remain below the barrier, but most stars are able to penetrate it, after which they are subject to RR and achieve a nearly thermal distribution of eccentricities. This process requires roughly 50 Myr in nuclear models with relaxed stellar cusps, or $\gtrsim 10$ Myr, regardless of the initial distribution of eccentricities, in nuclear models that include a dense cluster of $10 M_{\odot}$ black holes. We find a probability of $\lesssim 1\%$ for any S-star to be tidally disrupted by the SBH over its lifetime.

Subject headings: black hole physics-Galaxy:center-Galaxy:kinematics and dynamics-stellar dynamics

1. INTRODUCTION

Observations of the Galactic center (GC) reveal a cluster of about 20 stars, mainly main-sequence B stars, that extends outward to about a tenth of a parsec from the central supermassive black hole (SBH; Ghez et al. 2008). These stars, usually referred to as “S-stars,” follow orbits that are randomly oriented and have a nearly “thermal” distribution of eccentricities, $N(e)de \sim ede$ (Gillessen et al. 2009). The existence of such young stars so close to the GC SBH challenges our understanding of star formation since the strong tidal field of the SBH should inhibit the collapse and fragmentation of molecular clouds (Morris 1993). For this reason, it is usually assumed that the S-stars formed elsewhere and migrated to their current locations. However, the migration mechanisms proposed in the literature result in orbital distributions that differ substantially from what is observed. Post-migration dynamical evolution due to gravitational interactions with other stars or stellar black holes (BHs) has been invoked to bring the predicted orbital distributions more in line with observations (e.g., Merritt et al. 2009; Perets et al. 2009; Madigan et al. 2011; Zhang et al. 2012).

The S-stars approach closely enough to Sgr A* that relativistic corrections to their equations of motion can be important. In this paper, we apply recent insights about how relativity interacts with Newtonian (star-star) perturbations near Schwarzschild and Kerr SBHs. Using an approximate Hamiltonian formulation that includes a post-Newtonian description of the effects of relativity, we explore the evolution of the S-star orbits starting from

initial conditions that correspond to the different formation models proposed in the literature. Evolving the initial conditions for a time of the order the lifetime of the S-stars, and comparing with the observed distribution of orbital elements, allows us to place constraints on both the parameters of the nuclear cusp and the S-star origin models.

2. GRAVITATIONAL ENCOUNTERS NEAR THE SBH

Timescales of interest are of order 100 Myr, the main-sequence lifetime of a B star, or less. Such times are short compared with two-body (non-resonant, NR) relaxation times near the center of the Milky Way (e.g., Merritt 2010; Antonini & Merritt 2012), hence we ignore NR relaxation in what follows and assume that orbital energies, i.e. semi-major axes a , are unchanged once a star has been deposited near Sgr A*.

Resonant relaxation (RR) (Rauch & Tremaine 1996; Hopman & Alexander 2006) acts to change orbital eccentricities in a time

$$T_{\text{RR}} = \left(\frac{L_c}{|\Delta L_{\text{coh}}|} \right)^2 t_{\text{coh}}, \quad (1)$$

the “incoherent RR time,” where L_c is the angular momentum of a circular orbit having the same semi-major axis as the test star and t_{coh} is the “coherence time,” defined as the time for a typical field-star to change its orbital orientation; the latter is the shortest of the mass precession time (due to the distributed mass), the relativistic precession time (due to the 1PN corrections to the Newtonian equations of motion), and the time for RR itself to reorient orbital planes. For instance, in the

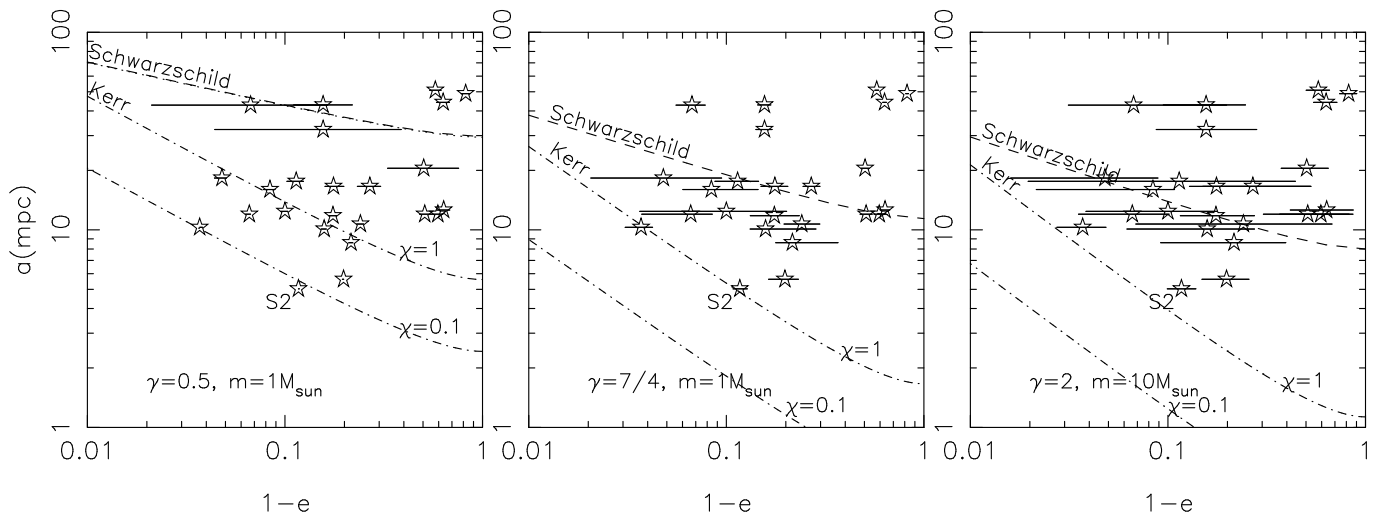


Figure 1. Location of the Galactic center S-stars on the (a, e) plane, compared with the Schwarzschild barrier (dashed line, equation 3), and the curve along which frame-dragging torques compete with \sqrt{N} torques from the stars (dash-dotted lines, equation 5, with two different values of the SBH spin χ). The three panels are for three models of the nucleus, as described in the text. The S-star data are from Gillessen et al. (2009). Horizontal tick marks give the expected amplitude of eccentricity changes as an orbit precesses in the fixed torquing field due to the field stars (equation 41 from Merritt et al. 2011).

case that field-star precession is dominated by relativity,

$$T_{\text{RR}} \approx \frac{3}{\pi^2} \frac{r_g}{a} \left(\frac{M_\bullet}{m} \right)^2 \frac{P}{N(<a)} \quad (2)$$

$$\approx 1.4 \times 10^5 \left(\frac{a}{10 \text{ mpc}} \right)^{1/2} \left(\frac{m}{1 M_\odot} \right)^{-2} \left(\frac{N}{10^3} \right)^{-1} \text{ yr}$$

where $r_g \equiv GM_\bullet/c^2$, P is the orbital period of the test star, $N(<a)$ is the number of field-stars with semi-major axes less than a , m is the mass of the field stars, and mpc is milliparsecs; $M_\bullet = 4 \times 10^6 M_\odot$ has been assumed.

RR ceases to be effective at changing the eccentricities of stars whose orbits lie below (at higher eccentricities than) the ‘‘Schwarzschild barrier’’ (SB), the locus in the (a, e) plane where relativistic precession of the test star acts in a time shorter than the time for the field-star torques to change L . The SB is defined approximately by (Merritt et al. 2011)

$$(1 - e^2)_{\text{SB}}^{1/2} \approx \frac{r_g}{a} \frac{M_\bullet}{m} \frac{1}{\sqrt{N(<a)}}. \quad (3)$$

Orbits above (at lower e than) the SB evolve in response to RR by undergoing a random walk in e . If such an orbit ‘‘strikes’’ the SB, it is ‘‘reflected’’ in a time of order the coherence time and random-walks again to lower e , in a time $\sim T_{\text{RR}}$, before eventually striking the SB again etc. Penetration of the SB from above can occur but only on a timescale that is longer than both the RR and NRR timescales (Merritt et al. 2011).

If a star should find itself *below* the SB, torques from the field stars are still able to change the orientation of its orbital plane (‘‘2d RR’’) even though changes in eccentricity are suppressed. The timescale for changes in orientation is

$$T_{2\text{dRR}} \approx \frac{P}{2\pi} \frac{M_\bullet}{m_\star} \frac{1}{\sqrt{N(<a)}} \quad (4)$$

$$\approx 9.4 \times 10^5 \left(\frac{a}{10 \text{ mpc}} \right)^{3/2} \left(\frac{m}{1 M_\odot} \right)^{-1} \left(\frac{N}{10^3} \right)^{-1/2} \text{ yr}$$

where again $M_\bullet = 4 \times 10^6 M_\odot$ has been assumed. However, 2dRR itself ceases to be effective for orbits that come sufficiently close to the SBH, where dragging of inertial frames by a spinning SBH induces Lense-Thirring precession with a period that is shorter than the time for 2dRR to randomize orbital planes. The condition for an orbit to be in this regime is (Merritt & Vasiliev 2012)

$$(1 - e^2)^3 \left(\frac{a}{r_g} \right)^3 \lesssim \frac{16\chi^2}{N(<a)} \left(\frac{M_\bullet}{m} \right)^2 \quad (5)$$

with $\chi \equiv cS/(GM_\bullet^2)$ the dimensionless spin of the SBH, and S the SBH spin angular momentum. We define a_K , the ‘‘radius of rotational influence’’ of the SBH, as the value of a that satisfies equation (5) with $e = 1$; a_K is roughly 1 mpc for the Milky Way assuming $\chi = 1$ (Merritt et al. 2010).

While the joint evolution of an ensemble of stars near a spinning SBH can only be convincingly treated using an N -body code, Monte-Carlo algorithms have been constructed that faithfully reproduce the eccentricity evolution of single (test) stars due to the dynamical mechanisms described above, assuming that $N(a, e)$ for the field-star distribution is not evolving. In this paper, we use an algorithm similar to that described by Merritt et al. (2011). The Hamiltonian that defines the test-star motion includes terms representing the effects of the spherically-distributed mass (which results in precession of the argument of periastron), 1PN (Schwarzschild), 1.5PN (Lense-Thirring) precession due to relativity and dipole and quadrupole order terms representing the torquing due to the finite- N asymmetry in the field-star distribution (which induces changes in all the orbital elements). The direction of the torquing field is changed smoothly with time and is randomized in a time of t_{coh} , as described in §VB of Merritt et al. (2011).

Above the SB, where test-star precession times are comparable with typical field-star precession times, the assumptions underlying the derivation of resonant relaxation are satisfied and the algorithm correctly reproduces

Table 1
 Origin models for the S-stars

	p^a					TDs ^b (%)
Binary Disruption						
Burst scenario ^c	5Myr	20Myr	50Myr	100Myr	200Myr	
$\gamma = 0.5; m = 1M_{\odot}$	7.41×10^{-14}	7.39×10^{-12}	2.01×10^{-10}	1.31×10^{-9}	9.36×10^{-9}	0
$\gamma = 7/4; m = 1M_{\odot}$	5.11×10^{-5}	0.176	0.765	7.93×10^{-2}	3.10×10^{-2}	1.9
$\gamma = 2; m = 10M_{\odot}$	0.593	0.296	0.239	0.160	0.201	0.36
Migration from gaseous disk^c						
	5Myr	20Myr	50Myr	100Myr	200Myr	
$\gamma = 0.5; m = 1M_{\odot}$	2.90×10^{-11}	9.57×10^{-10}	8.29×10^{-9}	3.62×10^{-7}	1.12×10^{-5}	0
$\gamma = 7/4; m = 1M_{\odot}$	3.12×10^{-9}	6.14×10^{-7}	4.06×10^{-5}	1.70×10^{-4}	1.37×10^{-3}	0.12
$\gamma = 2; m = 10M_{\odot}$	6.78×10^{-3}	3.76×10^{-2}	0.138	0.168	0.184	0.41
Binary Disruption						
Continuous scenario ^d	5Myr	20Myr	50Myr	100Myr	200Myr	
$\gamma = 0.5; m = 1M_{\odot}$	7.21×10^{-13}	6.41×10^{-13}	5.32×10^{-13}	1.33×10^{-13}	1.267×10^{-13}	0
$\gamma = 7/4; m = 1M_{\odot}$	3.14×10^{-5}	0.147	0.645	0.819	0.660	0.16
$\gamma = 2; m = 10M_{\odot}$	8.07×10^{-2}	0.108	0.410	0.499	0.310	0

^aProbability value of the 2 samples Kolmogorov-Smirnov test

^bPercentage of stellar tidal disruptions after 200 Myr

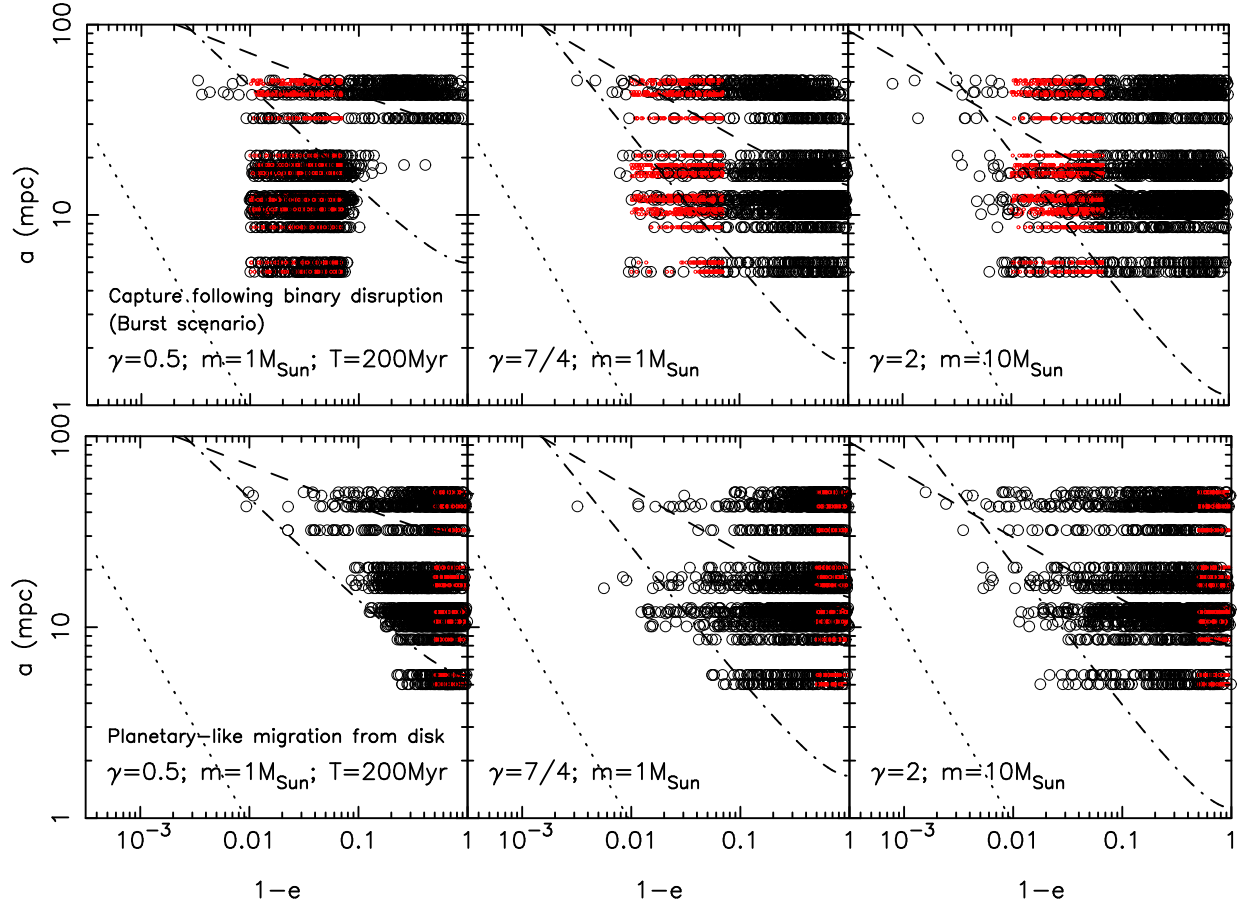
^cOrbits initialized at $t=0$
^dOrbits initialized at random times between [0,200 Myr]


Figure 2. Initial (red points) and final (black open circles, after 200 Myr) locations of the test particles in the Monte-Carlo integrations. Dashed and dot-dashed lines are defined in Figure 1; dotted lines give the tidal disruption radius of a $10 M_{\odot}$ star. Stars that initially have large eccentricities and lie near, but to the left of, the SB can penetrate the barrier and move to the right, where they remain. These stars end up with a nearly uniform distribution of angular momenta. Stars that are initially right of the SB tend to remain there, though some barrier penetration (from right to left) is observed near a_{crit} , the limiting value of a for which the SB exists.

the eccentricity evolution predicted by RR, as well as the “bounce” observed in N -body integrations when an orbit strikes the SB. For a test star that finds itself *below* the SB, the Schwarzschild precession time is short compared with field-star precession times. In this regime, a test star precesses with period close to

$$t_{\text{GR}} = \frac{P}{3} \frac{a}{r_g} (1 - e^2), \quad (6)$$

the 1PN apsidal precession time. During one precessional period, the field-star torques are nearly constant; as a result, the test-star’s angular momentum oscillates with period t_{GR} and with approximate amplitude (in the small- ℓ limit)

$$\Delta \ell \approx 2\ell_{\text{av}}^2 A_D \sin i, \quad (7a)$$

$$A_D = \frac{1}{3\sqrt{N(<a)}} \frac{M_\star(<a)}{M_\bullet} \frac{a}{r_g}. \quad (7b)$$

(Merritt et al. 2011). Here, $\ell^2 = 1 - e^2$, $M_\star(<a)$ is the mass in stars at radii $r \leq a$, and $\sin i$ specifies the inclination of the major axis of the torquing potential with respect to the orbit. By themselves, these periodic variations in e do not imply any directed evolution in angular momentum, but random switching of the direction of the torquing potential does result in a random walk in a test star’s angular momentum, allowing a star that is initially below the SB to approach it.

Dragging of inertial frames results in orbit-averaged rates of change of the argument of periastron, ω , and the angle of nodes, Ω , of the test star according to:

$$\left(\frac{d\Omega}{dt}\right)_{\text{FD}} = \frac{2G^2 M_\bullet^2}{c^3 a^3 (1 - e^2)} \chi, \quad (8a)$$

$$\left(\frac{d\omega}{dt}\right)_{\text{FD}} = -\frac{6G^2 M_\bullet^2}{c^3 a^3 (1 - e^2)} \cos i \chi. \quad (8b)$$

In equations (8), the “reference plane” for Ω and for i (the orbital inclination) is the SBH equatorial plane.

Since little is known about the distribution of stars and stellar remnants near the Galactic center, we explored a range of different models for the field-star distribution. Assuming a power-law density profile, the number of stars at radii less than r is

$$N(<r) = N_{0.2} \left(\frac{r}{0.2 \text{ pc}}\right)^{3-\gamma}, \quad (9)$$

where $N_{0.2} \equiv N(< 0.2 \text{ pc})$. The parameters $\{N_{0.2}, \gamma, m\}$ then uniquely define the background distribution in which the test particle orbits are evolved. In two models, we set $m = 1 M_\odot$, and we take either $\gamma = 0.5$ and $N_{0.2} = 8 \times 10^4$ (equation (5.247) in Merritt 2013), similar to what is inferred from observations (e.g., Do et al. 2009), or $\gamma = 7/4$ and $N_{0.2} = 1.6 \times 10^5$ (equation (5.246) in Merritt 2013), the expected values for a dynamically-relaxed population of stars (Bahcall & Wolf 1977). In another model, we adopt $N_{0.2} = 4.8 \times 10^3$, $\gamma = 2$ and $m = 10 M_\odot$. This latter choice of parameters approximately reproduces the density of stellar BHs predicted by collisionally relaxed models of a cusp of stars and stellar remnants around SgrA* (Hopman & Alexander 2006).

Figure 1 plots the S stars on the (a, e) plane, as well as the location of the SB; the latter depends on the parameters defining the nuclear cusp through equation (3). Dot-dashed lines in the figure delineate the region where frame-dragging torques from a spinning SBH would dominate stellar torques, equation (4). Particularly for large χ , many of the S stars lie close to this transition region, suggesting that frame dragging could be an important influence on their orbital evolution; for instance, by inhibiting 2dRR. This figure does not give information about timescales, but we note that characteristic times like T_{RR} are functions of the nuclear parameters, which can be important given the limited lifetimes of the S stars.

In the two models with a steep cusp, the SB delineates the boundary of the S-star orbits, with only a few stars lying below the minimum $a = a_{\text{crit}} \approx (M_\bullet/m\sqrt{N})r_g$ for which the barrier exists. In these models, the existence of the SB is expected to strongly influence the eccentricity evolution of at least some of the S stars; for instance, by limiting the maximum eccentricity attainable by a star that starts above the barrier. Furthermore, for some of the nuclear models, Figure 1 shows that some of the S-stars can lie both above a_{crit} and below the SB. Such a location would be highly unlikely, in a time as short as ~ 100 Myr, for stars that started above the SB, but is reasonable if the stars were placed initially on such orbits via one of the mechanisms described below.

3. FORMATION MODELS

We considered two models for the origin of the S stars.

- (1) Formation of the S-stars in binaries far from the center ($r > 0.1 \text{ pc}$). In this model, the binaries are scattered onto low-angular-momentum orbits that bring them close enough to the SBH that an exchange interaction can occur, leaving one star on a tightly-bound orbit around SgrA* (Hills 1998; Yu & Tremaine 2003; Antonini et al. 2010). The radius at which the SBH tidally disrupt a binary is typically a few tens of AU for main sequence binaries, and the orbital eccentricity is expected to be large. The initial orbital inclinations of the S-stars will be either randomly distributed if the binaries originated in an isotropic stellar cusp (Perets et al. 2007; Perets & Gualandris 2010) or highly correlated if they formed in a stellar disk (Madigan et al. 2009).
- (2) Formation of the S-stars in a disk at roughly their current radius, either one of the known stellar disks, or a pre-existing one. Formation in the disk would be followed by migration to their current locations. This model predicts initially small eccentricities and inclinations (Levin 2007).

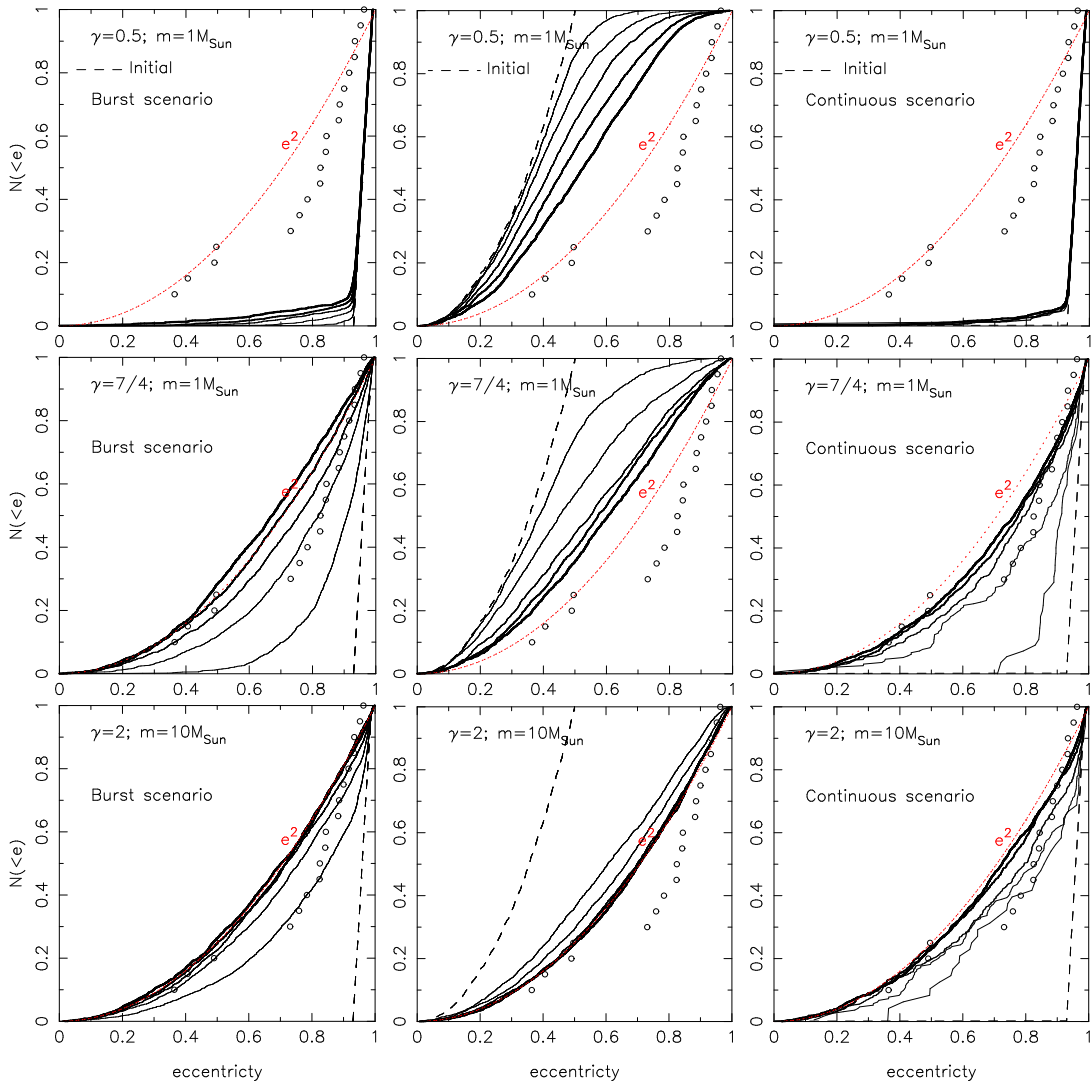


Figure 3. Cumulative distribution of eccentricities for different S-star formation models after 5, 20, 50, 100 and 200Myr (line thickness increases with time). Open circles give the observed distribution; dot-red line shows a “thermal” eccentricity distribution. Left and right panels correspond to formation through capture following binary disruption, middle panels to formation in a stellar disk followed by migration through interaction with a gaseous disk.

4. ORBITAL EVOLUTION

We start by assuming that $N(a)$ is known: it is given by the observed values of a . For each S-star (i.e. for each value of a), 100 Monte-Carlo experiments were carried out using the Hamiltonian model described above, in each of the three nuclear models, for an integration time of 200 Myr. The initial orbital eccentricities were assigned from a thermal distribution, $N(< e) \propto e^2$, over some specified range in e . In the case of migration from a gaseous disk we required $e \leq 0.5$ initially. When considering the binary disruption model, we only considered orbits with initial eccentricities in the range $0.93 \leq e \leq 0.99$. In this case, we assume either that the S-stars are brought to their current location at the same time (*burst scenario*) or that they arrive at random times between 0 and 200 Myr (*continuous scenario*). The former choice corresponds to a burst of S-star formation, for instance in a stellar disk (Madigan et al. 2009), while the latter choice assumes that the S-stars form continuously in the isotropic stellar cusp (Perets et al. 2007).

In all cases we set $\chi = 1$.

Stars were assumed to be tidally disrupted when they approached the SBH within a distance $r_t = 2R(M_\bullet/m)^{1/3}$ (Antonini et al. 2011a), with $m = 10 M_\odot$ and $R = 8 R_\odot$.

Figure 2 compares the initial and final (after 200 Myr) $a - e$ distributions. In the two, steep-cusp models with high initial e , most of the stars start off to the left of the SB, where evolution in angular momentum is strongly suppressed by the Schwarzschild precession. Nevertheless, it can be seen that, after some time, an initially eccentric population separates into two subpopulations: stars that are so far leftward of the SB initially that their eccentricities hardly evolve; and stars that either begin rightward of the SB, and remain there, or that are close enough initially to the barrier to cross it. The latter stars are subject to RR after crossing the barrier and end up with a nearly thermal eccentricity distribution. A clear “gap” between the two populations is evident in several of the frames of Figure 2; the gap extends from the SB

on the right, to a somewhat higher eccentricity on the left. The SB acts like a membrane that is permeable in one direction only, from left to right: having crossed the barrier from left to right, a star moves quickly (in a time of $\sim T_{\text{RR}}$) to a region of lower e where it remains¹. The observed evolution below the SB is due to reorientation of the torquing potential which results in a random walk in angular momentum, preferentially toward lower e (see §VB of Merritt et al. 2011); this mechanism is qualitatively similar to resonant relaxation but obeys a different set of relations (Alexander & Merritt 2012).

On the other hand, when eccentricities are initially low, as in the bottom panels of Figure 2, they tend to remain low, i.e., above the SB. As noted in Merritt et al. (2011), the permeability of the SB tends to increase near a_{crit} and this can be seen in Figure 2 as well.

Time evolution of the cumulative distribution of eccentricities is shown in Figure 3. (In this figure and in the analysis that follows, we do not include S-stars that likely belong to the disk(s) of O/WR stars, i.e. S66, S67, S83, S87, S96, S97). Eccentricity distributions were found to approach a nearly “thermal” form in a time of order T_{RR} . Based on Figure 3, we see that the lifetime of the S-stars may, or may not, be long enough for this to happen, depending on the nuclear model. We compared the results of the Monte-Carlo integrations with S-star data by performing 2-sample Kolmogorov-Simornov (K-S) tests on the e distributions (Table 1). The best match to observations is attained after 20 Myr of evolution in *stellar* cusp models in the continuous scenario with $\gamma = 7/4$ and starting from initially high eccentricities (K-S test p -values of ≈ 0.7). Integrations that include stellar BHs also generate orbital distributions which are in agreement with observations after approximately 5 and 20 Myr of evolution for initially high and low eccentricity distributions respectively.

We tested the degree of randomness of the orbital planes using the Rayleigh statistic \mathcal{R} (Rayleigh 1919), defined as the resultant of the unit vectors l_i , $i = 1 \dots N_{\text{mc}}$, where l_i is perpendicular to the orbital plane of the i_{th} star and N_{mc} is the total number of Monte-Carlo data points (i.e., $N_{\text{mc}} = 1900$). Since the test stars were initialized with the same inclination, the orbits are initially strongly correlated and $\mathcal{R} \approx N_{\text{mc}}$; over a time of order $T_{2\text{dRR}}$, 2dRR tends to randomize the orbital planes and \mathcal{R} approaches $\sqrt{N_{\text{mc}}}$, the value expected for a random distribution. When the main contribution to dynamical relaxation comes from stellar BHs, \mathcal{R} reached values consistent with isotropy after ~ 20 and ~ 50 Myr for initially high and low eccentricity distributions respectively. In the *stellar*-cusp model with $\gamma = 7/4$ and starting from initial high e , \mathcal{R} reached values consistent with isotropy after ~ 100 Myr, while in all the other stellar-cusp models we measured a significant departure from randomness ($\mathcal{R}/N_{\text{mc}} \gtrsim 0.2$) even after 200 Myr of evolution. We estimated \mathcal{R} separately for orbits that any time were below the dot-dashed lines of Figure 2 and found that this population had a distribution of orbital planes which was less consistent with being random. Evidently, 2dRR was somewhat inhibited by frame dragging for orbits with initially large eccentricities.

¹ This behavior has been confirmed via direct N -body integrations.

The fraction of stars that would have been tidally disrupted after 200 Myr of evolution was never larger than $\sim 1\%$ (Table 1). As a comparison, in purely Newtonian integrations, Perets et al. (2009) found that up to $\sim 30\%$ of stars were disrupted after 20 Myr of evolution.

5. CONCLUSIONS

In this paper we studied the combined effects of Newtonian and relativistic perturbations on the angular momentum evolution of the Galactic center (GC) S-stars. For the first time we have shown that the $a - e$ distribution of the S-stars predicted by the binary disruption model, in which the stars are delivered to the GC on high-eccentricity orbits, is consistent with the observed orbits even when relativistic effects are considered. In these formation models, most of the orbits lie initially below the Schwarzschild barrier, the locus in the (a, e) plane where resonant relaxation is ineffective at changing eccentricities. Contrary to this basic prediction, we found that orbits starting sufficiently close to the barrier are sometimes able to penetrate it, diffusing above and reaching a nearly thermal e -distribution; a small fraction of stars remain confined below the barrier at low angular momenta ($e \gtrsim 0.95$). A good match to observations is achieved after ~ 20 Myr of evolution if the distribution of field stars at the GC follows a nearly dynamically relaxed form. Models that include a mass-segregated population of stellar BHs also generate after ~ 10 Myr of evolution distributions that are marginally consistent with observations.

Based on the origin models considered here, the S-star orbits can only be reproduced by postulating dynamically relaxed states (i.e., steep density cusps) for the GC. This result is interesting given that such models are currently disfavored by observations (Buchholz et al. 2009; Do et al. 2009) and by some theoretical arguments (Merritt 2010; Antonini et al. 2011b; Gualandris & Merritt 2012).

DM was supported in part by the National Science Foundation under grant no. 08-21141 and by the National Aeronautics and Space Administration under grant no. NNX-07AH15G.

REFERENCES

- Alexander, T., & Merritt, D. 2012, in preparation
 Antonini, F., Faber, J., Gualandris, A., & Merritt, D. 2010, ApJ, 713, 90
 Antonini, F., Lombardi, J. C., Jr., & Merritt, D. 2011a, ApJ, 731, 128
 Antonini, F., Capuzzo-Dolcetta, R., Mastrobuono-Battisti, A., & Merritt, D. 2011b, ApJ, 750, 111
 Antonini, F. & Merritt, D. 2012, ApJ, 745, 83
 Bahcall, J. N., & Wolf, R. A. 1977, ApJ, 216, 883
 Buchholz, R. M., Schödel, R., & Eckart, A. 2009, A&A, 499, 483
 Do, T., Ghez, A. M., Morris, M. R., Lu, J. R., Matthews, K., Yelda, S., & Larkin, J. 2009, ApJ, 703, 1323
 Hills, J. G. 1988, Nature, 331, 687
 Hopman, C., & Alexander, T., 2006, ApJ, L645
 Ghez, A. M., et al. 2008, ApJ, 689, 1044
 Gillessen, S., Eisenhauer, F., Trippe, S., Alexander, T., Genzel, R., Martins, F., 2009, ApJ, 692, 1075
 Gualandris, A., & Merritt, D. 2012, ApJ, 744, 74
 Levin, Y. 2007, MNRAS, 374, L515
 Madigan, A., Levin, Y., & Hopman, C. 2009, ApJ, 697, L44
 Madigan, A., Hopman, C., & Levin, Y. 2011, ApJ, 738, 99

- Merritt, D., Gualandris, A., & Mikkola, S. 2009, *ApJ*, 693, 35
Merritt, D., 2010, *ApJ*, 718, 739
Merritt, D., Alexander, T., Mikkola, S., & Will, C. 2010, *PhRvD*, 81, 062002
Merritt, D., Alexander, T., Mikkola, S., & Will, C. 2011, *PhRvD*, 84, 4024
Merritt, D., 2013, *Dynamics and Evolution of Galactic Nuclei* (Princeton: Princeton University Press), p. 337.
Merritt, D., & Vasiliev, E. 2012, [arXiv:1208.6274](https://arxiv.org/abs/1208.6274)
- Morris, M. 1993, *ApJ*, 408, 496
Perets, H. B., Hopman, C., & Alexander, T. 2007, *ApJ*, 656, 709
Perets, H. B., Gualandris, A., Kupi, G., Merritt, D., & Alexander, T. 2009, *ApJ*, 702, 884
Perets, H. B., Gualandris, A. *ApJ*, 719, 220
Rauch, K. P., & Tremaine, S. 1996, *New Astronomy*, 1, 149
Rayleigh, L. 1919, *Phil. Mag.*, 37, 321
Zhang, F., Lu, Y., & Yu, Q. 2012, [arXiv:1210.1901](https://arxiv.org/abs/1210.1901)
Yu, Q., & Tremaine, S. 2003, *ApJ*, 599, 1129